Workshop on Computational Physics & Cellular Automata
Aug 8-11, Ouro Prêto, MG, Brasil, 1989

ASPECTS OF CLASSICAL EXCITATIONS IN TWO-DIMENSIONAL MAGNETIC SYSTEMS

G.M. Wysin
Department of Physics
Kansas State University
Manhattan, KS 66506 USA

ABSTRACT

Dynamic properties of classical spin excitations in models for quasi-two-dimensional materials are described. Included are spin configurations for vortex and vortex-like excitations from continuum limit equations of motion, together with comments about their stability. Models studied are the anisotropic ferro- and antiferromagnets, and an easy-plane ferromagnet with 4-fold in-plane symmetry breaking. Results from numerical simulations of the dynamic structure function $S^{\alpha\alpha}(\vec{k},\omega)$ are shown and compared with phenomenological theories.

1. INTRODUCTION

1.1 Low-Dimensional Models

Understanding the dynamic properties of excitations in magnetic models is a challenging and exciting enterprise, and from the theoretical viewpoint, analysis for systems in one or two dimensions can in many cases be carried out with more details than would be possible in three dimensions. From the experimentalists' perspective, there exist a wide variety of real materials which can be quite accurately described in terms of strong spin-spin interactions acting only along one or two of the crystal axes, thereby imposing a lower effective dimensionality.[1-4] For these materials, at temperatures above a transition temperature where the full three-dimensional interactions become relevant, the spin degrees of freedom can be described by a Hamiltonian with a lower effective dimensionality $d < 3$. Then the material is called "quasi-d-dimensional."

1.2 Quasi-One-Dimensional Magnets and Solitons

Historically, the most well known quasi-one-dimensional magnetic materials[1] are the spin-1 easy-plane ferromagnet $CsNiF_3$, and the spin-5/2 easy-plane antiferromagnet $(CH_3)_4NMnCl_3$, known as TMMC. These and

other materials have been thoroughly studied experimentally and analyzed in terms of nearest neighbor classical spin chain Hamiltonians possessing soliton modes.[5-7] The analysis of equilibrium and dynamic properties for such models is a mature and still active field (for example, see the article by D.P. Landau herein). Usually the interactions are anisotropic, perhaps with an Ising (easy-axis) or planar (easy-plane) symmetry. Presence of Ising anisotropy will lead to the possibility of static soliton-like excitations, involving rotations of the spin field through π, connecting regions having the two energetically equivalent alignments along the Ising axis. With planar anisotropy, there is the possibility of static soliton-like excitations involving in-plane rotations through 2π for ferromagnets or π for antiferromagnets. These typically will be better defined if there is a small applied magnetic field within the easy plane, breaking the symmetry in that plane.

Quite generally, with reasonable continuum limit assumptions, magnetic Hamiltonians in one dimension map approximately onto the one-dimensional sine-Gordon (sG) equation.[5-7] Therefore, phenomenological descriptions involve an "ideal gas" of sG solitons moving within (and perturbing) a background field of small amplitude spin waves.[8] Within this sG description, contributions to the dynamic structure function, $S^{\alpha\alpha}(\vec{k},\omega)$, as measured in inelastic neutron scattering, are expected due to solitons (peaks at $\omega = 0$), spin waves (peaks at finite ω) and multi-spinwave processes (which can also contribute to $\omega = 0$ intensity). In terms of gross features this description is probably valid for many materials. However, there are known difficulties. Corrections are expected due to deviations from sG dynamics.[9,10] The mapping onto the sG equation is approximate---spins tilt out of the easy plane for "planar" systems, an effect not fully accounted for in the sG equation. Also there could be quantum effects, and higher order soliton-spinwave interaction effects. However, if we consider quantum effects to be small (expected for $S \geq 1$), then numerical spin dynamics integrations are a productive way to avoid the sine-Gordon mappings and at the same time obtain accurate results for $S^{\alpha\alpha}(\vec{k},\omega)$. Conveniently, at this time available computing power is appropriate for performing these spin dynamics calculations for

reasonably large systems in two dimensions (100 x 100) as well as for one-dimension.

1.3 Quasi-Two-Dimensional Magnets and Vortices

Understanding of the statics and dynamics of quasi-two-dimensional magnets is not so thoroughly developed. However, the variety of challenging models and materials and possibilities for topological excitations is much greater than for one dimension. Some typical examples of quasi-two-dimensional magnets include[2] $BaCo_2(AsO_4)_2$, an XY ferromagnet, $BaNi(PO_4)_2$, an XY antiferromagnet, and Rb_2CrCl_4, an XY ferromagnet with in-plane symmetry-breaking.[3] Also, there is the nearly isotropic Heisenberg ferromagnet K_2CuF_4, and the XY ferromagnet $CoCl_2$ intercalated in graphite.[4] Among the available materials spin-S values range from 1/2 to 2, with interesting exchange and crystal field anisotropies on triangular, honeycomb and square lattices.

For two-dimensional models, in addition to spin waves and solitons (or now, "domain walls"), there can also be "vortex" excitations involving a singular point in the spin field, which has a nonzero curl. All of these can be expected to make contributions to $S^{\alpha\alpha}(\vec{k},\omega)$. The gross features should be well described by a phenomenological model, in terms of an ideal gas of walls, vortices, and spinwaves weakly interacting. For a simple model such as one with planar anisotropy but no applied fields (e.g., XY model), only vortices and spinwaves are present, and an ideal gas phenomenology has been developed by Mertens et al.[11] to describe the dynamics above the vortex unbinding[12] transition temperature (Kosterlitz-Thouless transition temperature T_{KT}). Static vortices are responsible for zero frequency intensity in $S^{\alpha\alpha}(\vec{k},\omega)$, that is, a central peak. The phenomenology can be compared with numerical simulations of $S^{\alpha\alpha}(\vec{k},\omega)$, however, an exact separation of central peak intensity into vortex and multi spinwave components is difficult. The numerical simulations suggest that corrections to the ideal gas phenomenology are needed, especially for the out-of-plane spin component correlations. However, for $T > T_{KT}$, the phenomenology assumes unperturbed vortices moving with a Boltzmann distribution of velocities, but at present it is not completely understood how strongly the vortex-spinwave or vortex-vortex interactions modify the

correlations, nor are the dispersion relation and velocity distribution of moving vortices actually known.

Ideally, one should consider the linearized perturbation about a vortex solution to obtain the vortex-spinwave scattering properties and vortex stability with respect to perturbations. In practice, this leads to a 4th order eigenvalue problem for which the bound states are not known. Instead, numerical integrations can be used, starting from a vortex initial condition, to indicate the dynamic stability. Similarly, numerical simulations have been used to indicate properties for travelling vortices. Any information about dynamic properties of isolated vortices obtained in this way will be helpful in improving phenomenological models, and offer guidance for other models involving more complex anisotropic interactions.

There are three primary goals for this paper: i) to review the classical mechanics description of spin waves, domain walls, and especially, vortices in several magnetic models; ii) to present some results relating to stability of vortices (as derived from continuum theory) when placed on a lattice; iii) to present results for $S^{\alpha\alpha}(\vec{k},\omega)$ for these models, in the light of available phenomenology theories. The models considered are the anisotropic Heisenberg model (ferro and antiferromagnetic exchange), and a model for Rb_2CrCl_4, which is an easy-plane ferromagnet with 4-fold in-plane symmetry breaking anisotropy. The intention is to give an idea of the remarkable assortment of excitations in the various models, concentrating on their spin configurations, stability and dispersion properties, and the implications of these for their contributions to dynamic space-time correlation functions.

2. ANISOTROPIC HEISENBERG MODELS: XY TO ISOTROPIC FERROMAGNETS

For spin variables $\vec{S}_i$, where i labels a lattice site in two dimensions, a simple Hamiltonian is

$$H = - J \sum_{(i,j)} (S_i^x S_j^x + S_i^y S_j^y + \lambda S_i^z S_j^z) , \qquad (1)$$

where the sum is over nearest neighbor pairs (i,j) and the parameter λ measures the degree of exchange anisotropy. Here we consider only planar

anisotropy, with $0 \leq \lambda \leq 1$. As λ ranges from 0 to 1 the model changes smoothly from the XY model to the isotropic Heisenberg model.

The discrete equations of motion resulting from (1), obtained most easily through classical Poisson brackets, are

$$\frac{d\vec{S}_i}{dt} = \vec{S}_i \times \vec{F}_i \tag{2}$$

$$\vec{F}_i = J \sum_{(i,j)} (S_j^x \hat{x} + S_j^y \hat{y} + \lambda S_j^z \hat{z}). \tag{3}$$

The sum in (3) involves only the nearest neighbors of site i. This form of the differential equations is used for numerical integrations due to its simplicity and lack of trigonometric function evaluations. Using these equations, and assuming small dynamic fluctuations from a state with $\vec{S}=S(1,0,0)$ leads to the spinwave dispersion relation for an excitation with wavevector (k_x,k_y),

$$(\omega/2JS)^2 = (2-c)\ (2-\lambda c); \quad c \equiv \cos k_x a + \cos k_y a \tag{4}$$

where a is the lattice spacing. This dispersion has an interesting feature. For small wavevectors, we have

$$\omega \approx JS(ka)^2 \qquad \text{for} \qquad \lambda = 1 \text{ (Heisenberg)} \tag{5}$$

$$\omega \approx 2JS(ka) \qquad \text{for} \qquad \lambda = 0 \text{ (XY)}. \tag{6}$$

This point is that for intermediate values of λ, there is a mixture of linear and quadratic wavevector dependencies, with a crossover from linear to quadratic k-dependence at adequately large k.

2.1 A Continuum Limit

A crossover effect for the continuum solutions as λ ranges from 0 to 1 might also be expected, especially since a planar vortex is not expected for the isotropic model. The continuum limit[13] can be studied by using spin variables in terms of the spherical coordinates:

$$\vec{S}(\vec{r}) = S(\cos\theta\cos\phi,\ \cos\theta\sin\phi,\ \sin\theta). \tag{7}$$

In a lowest order continuum limit derived from a square lattice, the coupled equations of motion for the $\theta(\vec{r})$ and $\phi(\vec{r})$ fields are

$$\dot{\theta} = JS\ (\cos\theta\ \nabla^2\phi - 2\sin\theta\ \vec{\nabla}\phi\cdot\vec{\nabla}\theta) \tag{8}$$

$$\dot{\phi}\cos\theta = -JS\ \{[|\nabla\theta|^2 + |\nabla\Phi|^2 - 4 + \lambda\ (4-|\nabla\theta|^2)]\ \sin\theta\ \cos\theta + (\sin^2\theta + \lambda\ \cos^2\theta)\ \nabla^2\theta\} \tag{9}$$

These equations have two types of soliton-like <u>vortex</u> solutions[14] (or, an "instanton" when $\lambda = 1$).

2.2 Planar Vortices

Angle ϕ measures the spin angle projected on the easy xy plane, while angle θ measures the tilting of the spins up out of the xy plane. In the XY limit one expects a static planar solution, with $\theta = 0$ and $\dot{\theta} = \dot{\phi} = 0$. This exactly satisfies (9) and then (8) simplifies to the Laplace equation, for any value of λ:

$$\nabla^2\phi = 0\ . \tag{10}$$

This has a simple "planar vortex" (or antivortex) solution

$$\phi = \pm\ \tan^{-1}\ (y/x) + \phi_o$$
$$\theta = 0 \tag{11}$$

where ϕ_o is an arbitrary constant. The energy depends logarithmically on the system size R and a short distance cut-off r_a,

$$E_{pl} = \pi\ JS^2\ \ln(R/r_a). \tag{12}$$

This is the well known vortex (antivortex) of the XY model, but it also exists for nonzero λ. The vortex is singular at its center; the spin direction is undefined there. The antivortex differs from the vortex only in the sense of the circulation in the spin field.

In a system in thermodynamic equilibrium, it is expected that these are created as vortex-antivortex pairs, where the cost in energy depends logarithmically on the separation of their centers. In the Kosterlitz-Thouless transition for the XY model, it becomes possible to lower the free energy by creating pairs when the creation energy ΔU_{pair} can be counterbalanced by the entropy term $T\Delta S_{pair}$. This occurs at a transition temperature[15] $T_{KT} \approx 0.8\ JS^2$ for $\lambda=0$. It is useful to see whether

peculiarities of the classical magnetic Hamiltonian may affect this transition, and consider the dynamic signatures of the unbinding vortices.

2.3 Out-Of-Plane Vortices

It can be seen that equations (8) and (9) admit another static vortex solution,[13,14] possessing a nonzero out-of-plane component θ. With the in-plane angle ϕ given by (11), one can find asymptotic solutions to (9) with the following behaviors for small r and large r:

$$\sin\theta \approx \pm S\,[1 - \tfrac{1}{2}\, a\, (r/r_v)^2] \qquad r \to 0 \tag{13}$$

$$\sin\theta \approx \pm bS\, (r_v/r)^{1/2}\ \exp(-r/r_v) \qquad r \to \infty\ . \tag{14}$$

Here a and b are constants, and r_v is an effective "vortex radius"

$$r_v = \frac{1}{2}\left(\frac{\lambda}{1-\lambda}\right)^{1/2}\ . \tag{15}$$

This vortex is not singular at its center; the spins point along the z-axis at the center, with the z-component dying off exponentially away from the center over a length scale r_v. This configuration is called an "out-of-plane vortex."

Although an exact analytic expression for the out-of-plane vortex is not known, Gouvea et al.[14] have made an approximate evaluation of its energy E_{out}. The result is that for $\lambda \ll 0.8$, the planar vortex is energetically favorable; $E_{pl} < E_{out}$. But for $\lambda > 0.8$, the relationship is reversed; $E_{pl} > E_{out}$. This is an intriguing result; for a given value of λ, are both types of vortices possible, or is only the energetically favorable type dynamically allowed?

2.4 Vortex Dynamic Stability

One way to answer this question is to assume perturbations $\tilde{\theta}$ and $\tilde{\phi}$ about the known vortex solutions, and linearize the equations of motion in these perturbations, obtaining a pair of coupled linear differential equations for $\tilde{\theta}$ and $\tilde{\phi}$. These will be in the form of an eigenvalue problem, whose bound state solutions with negative energies will

correspond to instabilities of the original unperturbed vortex. If no negative energy bound states exist then the vortex is stable. Unfortunately, the eigenvalue problem cannot be solved for the case of the planar vortex, nor even set up for the out-of-plane vortex.

An alternative is to make a numerical integrations of the equations of motion, using a continuum vortex solution discretized on a lattice as the initial condition. A Landau-Gilbert damping term can be added to the equations of motion, to take up excess energy and reduce the effects of putting a continuum solution for an infinite system on a finite sized lattice. The equations of motion become

$$\frac{d\vec{S}_i}{dt} = \vec{S}_i \times \vec{F}_i - \epsilon \vec{S}_i \times (\vec{S}_i \times \vec{F}_i) \tag{16}$$

with $\vec{F}_i$ given in (3) and ϵ is the damping strength. Integrations were done[14] on a 40 x 40 lattice, with Neumann or free boundary conditions and a 4th order Runge-Kutta scheme, time step 0.04. The equations were integrated out to several hundred units with damping ϵ=0.1, starting from a planar vortex initial condition for a set of values $0 \leq \lambda \leq 1$. On a square lattice, for $\lambda < 0.72$, the planar vortex is found to be stable under these conditions (θ remains zero everywhere). For $\lambda \geq 0.72$, the simulation produces a striking destabilization of the planar vortex into an out-of-plane vortex, as seen in Figure 1. Similar results were obtained by repeating the simulations on triangular and hexagonal lattices. On the triangle lattice (coordination number z = 6) the planar vortex becomes unstable at $\lambda \approx 0.62$, and on the hexagonal lattice (z = 3) the planar vortex becomes unstable at $\lambda = 0.86$. The stability of the planar vortex is diminished by increasing coordination number and is strongly affected by the discreteness of the lattice.

A comparable set of simulations using the approximately known out-of-plane vortex as initial condition led to the same conclusion; there is a crossover value λ_c, below which only planar vortices are stable and above which only out-of-plane vortices are stable. These statements are also true for vortices in the XY antiferromagnet on a square lattice, where we find $\lambda_c \approx 0.71$. These results are especially relevant for

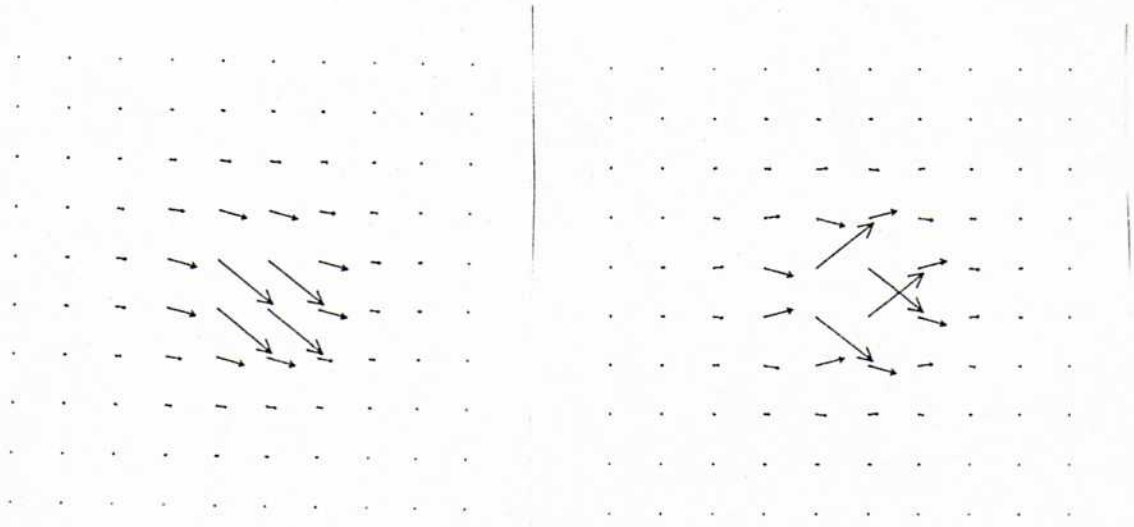

Figure 1. S^z spin components for out-of-plane vortices, with λ=0.80, for a) ferromagnet, b) antiferromagnet. The lengths of the arrows are proportional to the out-of-plane angle θ; the arrows are oriented at angle θ with respect to horizontal in the diagram. Note the antisymmetry of the antiferromagnetic vortex.

phenomenological calculations of the vortex contribution to the z-component spin-spin correlation functions.

2.5 Moving Vortices

It is useful to consider spin profiles for moving vortices, based on ideas from one-dimensional soliton dynamics. Boosting a static sG soliton for an easy-plane ferromagnet, which has $S^z = 0$, results in a profile with $S^z \sim \dot{\phi} = -v\phi_x$. The out-of-plane component is proportional to the soliton velocity v and the spatial derivative of ϕ. Generalizing to two dimensions, a planar vortex boosted along the x-direction should have

$$S^z \sim -v\phi_x = \frac{vy}{r^2} \tag{17}$$

or, for a vortex moving along an arbitrary direction, this is

$$S^z = -\frac{\vec{v} \cdot \hat{e}_\alpha}{4(1-\lambda)JSr} \quad , \quad \text{for } r \to \infty \tag{18}$$

where (r,α) are polar coordinates. This is an approximate far-field solution. Probably effects of discreteness can strongly affect the vortex core, and an adequate $r \to 0$ solution is not known. However, it is important to note the symmetry of the moving planar vortex. It is antisymmetric about a line through the center in the direction of the velocity. Along this line S^z changes sign. The presence of nonzero z components implies that moving planar vortices will contribute to $S^{zz}(\vec{k},\omega)$.

3. NUMERICAL CALCULATIONS OF $S^{\alpha\alpha}(\vec{k},\omega)$

Kawabata and Bishop[15] introduced a convenient combined Monte Carlo-molecular dynamics technique for performing microcanonical ensemble spin dynamics calculations. First, a Monte Carlo (MC) simulation (canonical ensemble) is used to generate a set of equilibrium configurations for a chosen temperature. Then these configurations can be used in an energy-conserving numerical integration of the spin dynamics equations of motion, written most efficiently in terms of the xyz spin components.

Typical simulations[11,14,16] reviewed here involved a 100 x 100 square lattice, with periodic boundary conditions. The system was considered to have two sublattices. In the MC algorithm all spins on one sublattice were updated simultaneously, so that the algorithm could be vectorized. Individual spins were updated in one of two ways: i) by using trial spins uniformly distributed on the units sphere, or, ii) by adding small increments to the old spin position, scaled by a parameter ℓ, and adjusting the length ℓ to give an acceptance rate from 30% to 40%. The former worked well for higher temperatures, the latter was more efficient for lower temperatures but may not be recommended for extremely low temperature. Most interest was in $T/J \gtrsim 0.5$, where J is the near neighbor exchange, so low temperatures were not a problem. About 2000 passes through the lattice were used to equilibrate the system, with the temperature slowly lowered to the desired value exponentially, in the sense of simulated annealing. Then, about 10,000 passes were used to generate an initial state for the spin dynamics, and for computing equilibrium averages.

In the spin dynamics part of the simulation, a 4th order Runge-Kutta integrator with fixed time step of 0.04 was used. The spin configuration

(or, selected components of its spatial Fourier transform) was sampled every m time steps, with m chosen from 1 to 32 depending on the frequencies of interest. A set of 512 samples were taken, to take advantage of a fast Fourier transform. Time-displaced correlations of the spatial Fourier transform of $\vec{S}(\vec{r},t)$, that is, $C^{\alpha\alpha}(\vec{k},\tau) = \langle S^{\alpha}(\vec{k},t)\ S^{\alpha}(\vec{k},t+\tau)\rangle$ were formed; the average is over initial times t, assuming periodic boundary conditions in time over an interval $\Delta t = 512 \cdot m \cdot 0.04$. The correlation $C^{\alpha\alpha}$ was multiplied by a Gaussian window function for smoothing the effects of the finite time interval; then the product was Fourier transformed with respect to the time displacement τ, thereby producing the dynamic structure function $S^{\alpha\alpha}(\vec{k},\omega)$.

Finally, the entire process described above was repeated 3 to 5 times and the set of results were averaged together to give $S^{\alpha\alpha}(\vec{k},\omega)$. The result was then plotted and analyzed in terms of central peak and spin wave components, characterized by appropriate intensities and widths.

3.1 Numerical Results for Dynamic Correlations: XY Model

Some results for the correlations $S^{\alpha\alpha}(\vec{k},\omega)$ for ferromagnetic and antiferromagnetic XY models are shown in Figures 2 and 3. In both cases the obvious feature is development of central peak intensity with increasing temperature, which is attributed to the unbinding of vortex-antivortex pairs. At the same time a softening and broadening of the spinwave peak occurs. For the ferromagnet, the width and intensity of the central peak has been compared with predictions of the ideal gas theory.[11] For the antiferromagnet, the optical spinwave appears in the S^{xx} correlation function, and there is a broad background intensity with frequencies ranging up to the spinwave frequency, while the acoustic spinwave appears in S^{zz} (see next section).

4. ANISOTROPIC HEISENBERG ANTIFERROMAGNETS

Reconsider model (1), but with antiferromagnetic exchange:

$$H = J \sum_{(i,j)} (S_i^x S_j^x + S_i^y S_j^y + \lambda S_i^z S_j^z) \qquad (19)$$

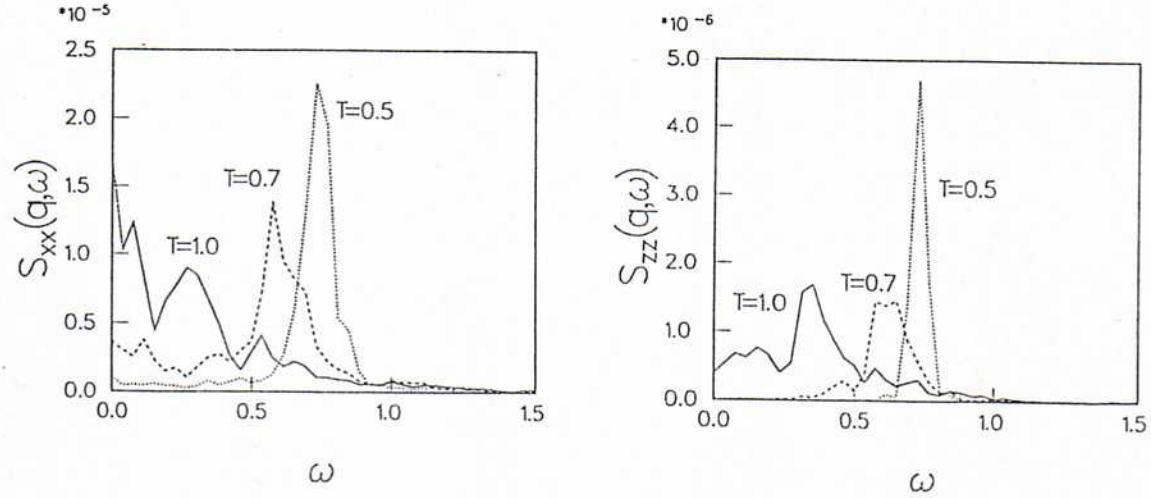

Figure 2. Correlation functions of in-plane and out-of-plane components for the XY ferromagnet at wavevector $\vec{k}a = (0.1,0.1)\pi$, from MC-MD simulations described in the text (J=1).

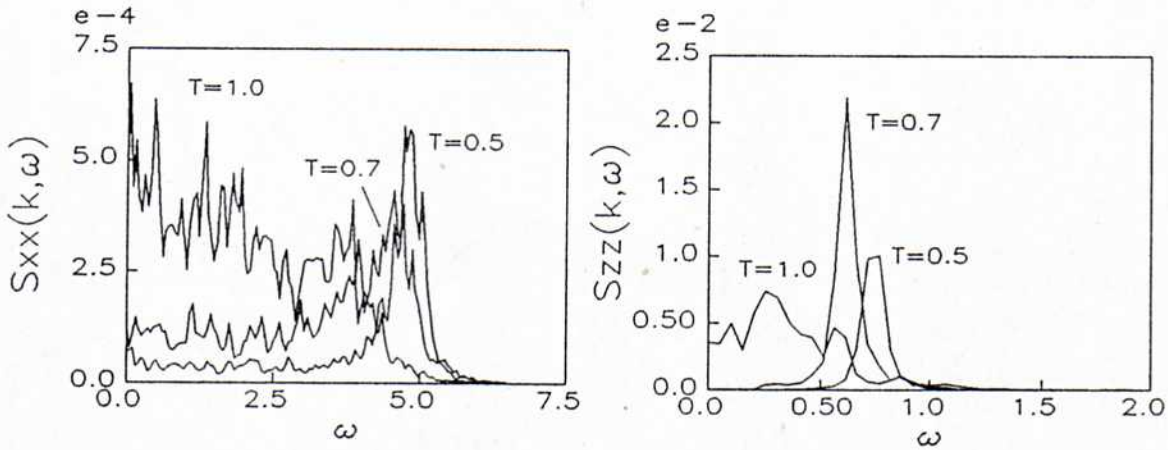

Figure 3. Correlation functions of in-plane and out-of-plane components for the XY antiferromagnet at wavevector $\vec{k}a = (0.1,0.1)\pi$, from MC-MD simulations described in the text. The acoustic spinwave appears in S^{zz}; the optical spinwave appears in S^{xx}.

with $J > 0$ here. The discrete equations of motion are given by equations (3) and (4) but with the spin of J reversed (equivalent to reversing the time axis). Now, the spinwaves are fluctuations from a ground state with alternating up/down spins on the two sublattices, e.g., $\vec{S}_A = S(1,0,0)$, $\vec{S}_B = S(-1,0,0)$. The spinwave dispersion then generally has two branches:

$$(\omega/2JS)^2 = (4-\lambda c^2) \pm 2(1-\lambda)c \; ; \; c \equiv \cos k_x a + \cos k_y a \qquad (20)$$

with +/- corresponding to optical/acoustic branches. For $\lambda \neq 1$, the symmetry of these modes is such that only the optic mode is seen in $S^{xx}(\vec{k},\omega)$, and only the acoustic mode is seen in $S^{zz}(\vec{k},\omega)$. However, for $\lambda=1$, the branches are degenerate and this distinction disappears.

4.1 A Continuum Limit: Heisenberg Model $\lambda=1$

A continuum limit can be made following Mikeska[6] in terms of four fields Θ, Φ, θ, ϕ, assuming fluctuations from an antiferromagnetic configuration,

$$\vec{S}_{\substack{A\\B}} = \pm S\,[\cos(\Theta\pm\theta)\cos(\Phi\pm\phi),\ \cos(\Theta\pm\theta)\sin(\Phi\pm\phi),\ \sin(\Theta\pm\theta)] \qquad (21)$$

and then the isotropic equations of motion, assuming small spatial derivatives and $\theta \ll 1$, $\phi \ll 1$, are

$$\dot{\Theta}/JS = -8\phi\cos\Theta \qquad (22)$$

$$\dot{\theta}/JS = \cos\Theta\,\nabla^2\Phi - \sin\Theta\,[2\vec{\nabla}\Theta\cdot\vec{\nabla}\Phi - 8\theta\phi] \qquad (23)$$

$$\dot{\Phi}/JS = 8\theta\sec\Theta \qquad (24)$$

$$\dot{\phi}/JS = \sin\Theta\,[8\theta^2\sec^2\Theta - 8\phi^2 - |\nabla\Phi|^2] - \sec\Theta\,\nabla^2\Theta\ . \qquad (25)$$

For static solutions, $\theta = \phi = 0$, and the equations for Θ and Φ are identical to those for the ferromagnet (this is true for any λ). Therefore, static antiferromagnet topological excitations are the same as those in the ferromagnet. For example, we can have the "instanton" solutions[17]

$$\Phi = \tan^{-1}(y/x); \qquad \sin\Theta = \frac{w^2-r^2}{w^2+r^2} \qquad (26)$$

where w is an arbitrary width parameter, and this configuration has finite energy $E = 4\pi JS^2$, independent of w and the system size! In thermal equilibrium there can be a small population of instantons in a background field dominated by spinwaves, with both making contributions[18] to $S(\vec{k},\omega)$. Theoretical models[19,20] for the finite temperature spinwave contribution have been developed, especially for wavevectors near the antiferromagnetic Bragg point $\vec{k}a = (\pi,\pi)$. For comparison, some numerical simulation results[21] are shown in Figure 4. These responses fit well to a product

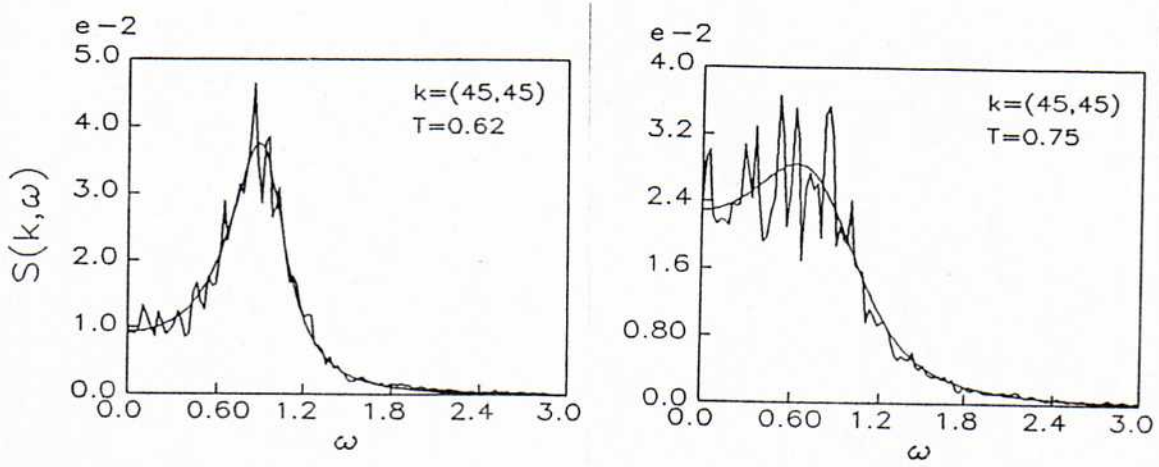

Figure 4. $S(\vec{k},\omega)$ for the Heisenberg antiferromagnet at wavevector $\vec{k}a = (45,45)\pi/50$ (from 100 x 100 lattice), from MC-MD simulations. The smooth curves are least squares fits using products of Lorentzians. Such fits account for most of the ω=0 intensity.

of Lorentzians, symmetrically located at positive and negative frequencies. Spinwave linewidths and frequencies from such fits are shown in Figure 5. Softening and broadening with increasing temperature are readily seen. These results are consistent with the dynamic scaling theory of Chakravarty et al.[19] Further details of these simulations will be published elsewhere.

5. A MODEL FOR Rb_2CrCl_4: IN-PLANE SYMMETRY-BREAKING

Hutchings et al.[3] has studied the compound Rb_2CrCl_4 using neutron scattering, and designed the following two-sublattice model Hamiltonian on a square lattice:

$$H = - J \sum_{(i,j)} \vec{S}_{i1} \cdot \vec{S}_{j2} + \sum_i D[(S^z_{i1})^2 + (S^z_{i2})^2] - \sum_i P\,[(S^x_{i1})^2 + (S^y_{i2})^2] \qquad (27)$$

The indices 1 and 2 refer to even and odd sublattices. The model includes ferromagnetic exchange J, easy-plane anisotropy D, and most importantly, an Ising anisotropy P which is sublattice-dependent. P reflects the crystal field effects of the Cl^- ions on the magnetic Cr^{++} ions. On the "1" sublattice, the Cl^- ions are closer to the Cr^{++} ions measuring along the y-axis, and on the "2" sublattice, the Cl^- ions are closer to the Cr^{++}

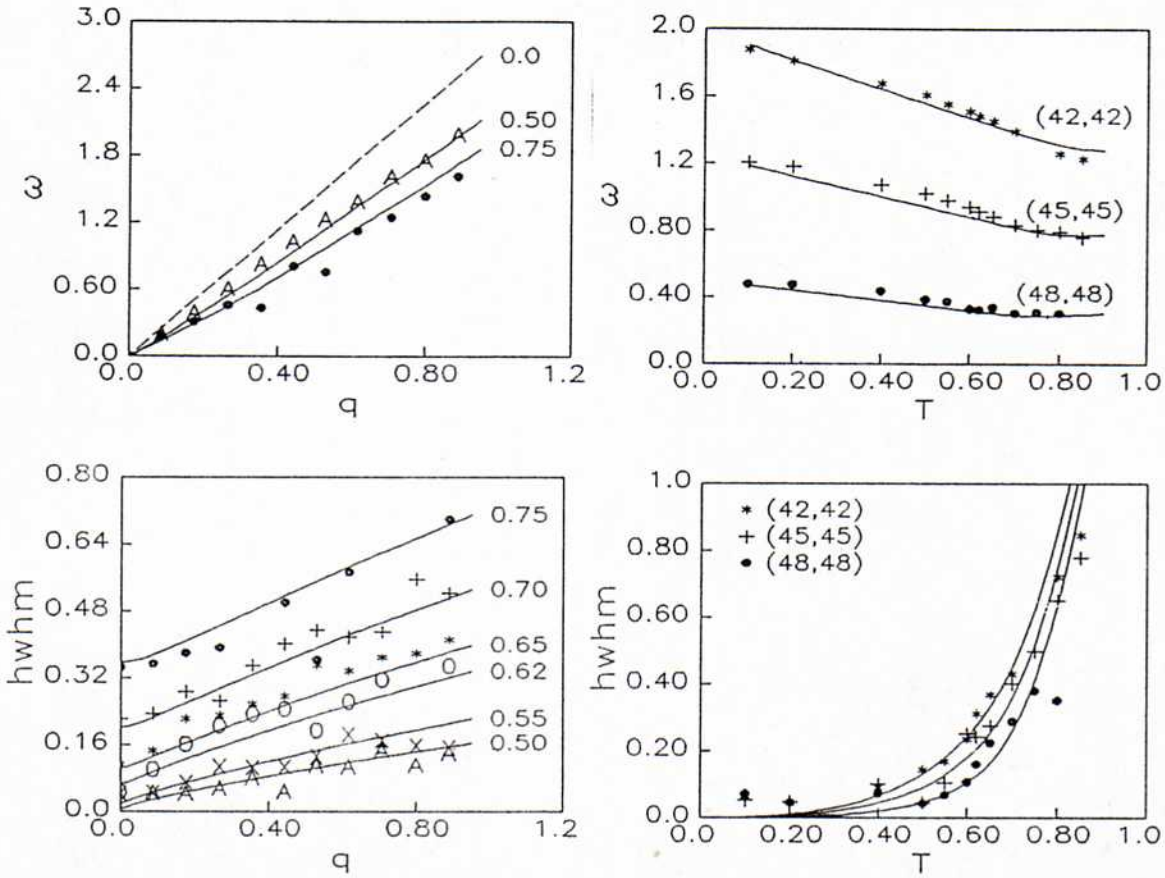

Figure 5. MC-MD data for spinwave frequencies (ω) and linewidths (hwhm) for the Heisenberg antiferromagnet, a) versus reduced wavevector $q = |\vec{k}-(\pi,\pi)|$ and b) versus temperature T. Curves in a) are labeled by various temperatures, curves in b) are labeled by wavevectors in units of $\pi/50a$. Solid curves correspond to a fit to the theory of reference 19, using parameters δ=2.5, γ_o=1.7, μ=1.7 and θ=0.7.

ions measuring along the x-axis. Therefore the Ising axes of the two sublattices are perpendicular. When competing with the nearest neighbor exchange, this results in an approximate 4-fold anisotropy within the easy (XY) plane. José et al.[22] have suggested that a 4-fold in-plane symmetry breaking (p = 4) is a borderline case for Kosterlitz-Thouless transitions. it is expected that XY-like systems with $p < 4$ will not show a KT transition, while $p > 4$ systems will, making Rb_2CrCl_4 an interesting system to consider.

5.1 A Continuum Limit

Following the method used for antiferromagnets, spins on the two sublattices are parameterized as[16]

$$\vec{S}_{\frac{1}{2}} = S[\cos(\Theta \pm \theta)\cos(\Phi \pm \phi),\ \cos(\Theta \pm \theta)\sin(\Phi \pm \phi),\ \sin(\Theta \pm \theta)]. \tag{28}$$

Assuming small spatial derivatives and $\theta \ll 1$, $\phi \ll 1$, the resulting equations of motion have planar solutions which satisfy (with $\Theta = \theta = 0$)

$$\Phi = \pm \pi/4,\ \pm 3\pi\ 4; \qquad \phi = (P/8J)\ \sin 2\Phi. \tag{29}$$

These represent the 4 possible local ground state configurations (or, 4 possible domain orientations). Another planar solution exists, where Φ must satisfy[16]

$$\nabla^2\Phi - \frac{1}{4D'JS^2}\ \ddot{\Phi} = \frac{1}{2}\left(\frac{P}{4J}\right)^2 \sin 4\Phi \tag{30}$$

where $D' = D + P/2$. This is a time-dependent sG equation in the variable 4Φ. A static vortex-like solution given by Hudak,[23] is a synthesis of a vortex circulation constrained by the 4-fold domain pattern at large distances (see Figure 6),

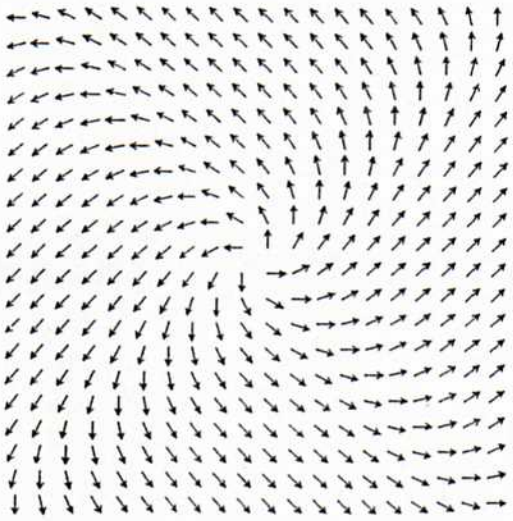

Figure 6. The 4-fold-symmetric domain-vortex of Equation (31), for P/J=1.0, n=1.

$$\Phi = \pm \tan^{-1} \{ \sinh[\frac{P}{2J} (y-y_o)]/\sinh [\frac{P}{2J} (x-x_o)]\} + n\pi/4 \qquad (31)$$

where n is an odd integer. This configuration, consisting of four domains separated by $\pi/2$ walls, has an energy which is linearly proportional to the system size (i.e., proportional to the length of the walls), in contrast to the logarithmic size dependence for the vortex in the XY model. However, a vortex-antivortex pair has a finite energy which is linearly proportional to the separation. As a result entropy and energy arguments for transitions in this system could be considerably modified from the XY model results. There are some numerical simulation data available from Gouvea et al.,[16] but the effects of the degree of symmetry-breaking and the freedom of out-of-plane spin components on KT transitions has not been clarified.

6. SUMMARY AND OUTLOOK

The rich variety of possible magnetic models in two dimensions gives remarkable opportunities for investigating dynamics of nonlinear excitations, including domain walls, vortices, instantons, and their subsequent effects on spinwaves. In addition, in-plane anisotropy and applied fields modify the vortex shape and dynamics, for example, as in Rb_2CrCl_4. Anisotropies and out-of-plane spin components are expected to modify vortex unbinding transitions but the details are not understood.

In the anisotropic Heisenberg models (both signs of J), there are planar and out-of-plane vortices; for a given anisotropy strength λ only one type will be stable. The planar vortex is unstable for λ greater than a crossover value λ_c, and the out-of-plane vortex is unstable for $\lambda < \lambda_c$.

In the Hutchings model for Rb_2CrCl_4, the competition between exchange and the sublattice-dependent Ising anisotropy leads to a special vortex-like excitation which might be called a "domain-vortex." It is a 4-domain coherent structure terminated in a singular point with a vortex core.

Further understanding of these and related systems will act as a foundation for investigating coherent dynamical modes, such as those involved in driven systems and in pattern formation.

Acknowledgement

The hospitality of Universidade Federal de Minas Gerais, where I had many beneficial discussions with M.E. Gouvêa and A.S.T. Pires, is greatly appreciated.

REFERENCES

1. Steiner, M., Kakuri, K. and Kjems, J.K., Z. Phys. B53, 117 (1983); Boucher, J.P., Regnault, L.P., Rossat-Mignod, J., Renard, J.P., Bouillot, J., Stirling, W.G. and Mezei, F., Physica 120B, 241 (1983).
2. Regnault, L.P. and Rossat-Mignod, J., in Magnetic Properties of Layered Transition Metal Compounds, editors de Jongh, L.J. and Willett, R.D. (Reidel, Dordricht, 1987).
3. Hutchings, M.T., Als-Nielsen, J., Lindgard, P.A. and Walker, P.J., J. Phys. C: Solid State Phys. 14, 5327 (1981).
4. Elahy, M. and Dresselhaus, G., Phys. Rev. B30, 7225 (1984).
5. Mikeska, H.J., J. Phys. C11, L29 (1978).
6. Mikeska, H.J., J. Phys. C13, 2913 (1980).
7. Bishop, A.R. and Schneider, T. (eds.) Solitons in Condensed Matter Physics, Springer-Berlin (1978).
8. Currie, J.F., Krumhansl, J.A., Bishop, A.R. and Trullinger, S.E., Phys. Rev. B22, 477 (1980).
9. Kumar, P., Phys. Rev. B25, 483 (1982); Physica 5D, 359 (1982); Magyari, E. and Thomas, H., Phys. Rev. B25, 531 (1982); J. Phys. C16, L535 (1983).
10. See Nonlinearity in Condensed Matter, edited by Bishop, A.R., Campbell, D.K., Kumar, P. and Trullinger, S.E., p. 24-80, Springer-Verlag (1987).
11. Mertens, F.G., Bishop, A.R., Wysin, G.M. and Kawabata, C., Phys. Rev. Lett. 59, 117 (1987), Phys. Rev. B39, 591 (1989).
12. Kosterlitz, J.M. and Thouless, D.J., J. Phys. C: Solid State Phys. 6, 1181 (1973); in Progress in Low Temperature Physics, edited by Brewer, D.F., Vol. 7B, Chap. 5 (North-Holland, Amsterdam, 1978).

13. Hikami, S. and Tsuneto, T., Prog. Theo, Phys. 63, 387 (1980).
14. Gouvêa, M.E., Wysin, G.M., Bishop, A.R. and Mertens, F.G., Phys. Rev. B39, 11840 (1989); in Computer Simulation Studies in Condensed Matter Physics, edited by Landau, D.P., Mon, K.K. and Schüttler, H.B., Springer-Verlag (1988).
15. Kawabata, C. and Bishop, A.R., Solid State Commun. 42, 595 (1982); ibid, 60, 169 (1986).
16. Gouvêa, M.E., Wysin, G.M., Bishop, A.R. and Mertens, F.G., J. Phys.: Condens. Matter 1, 4387 (1989).
17. Trimper, S., Phys. Lett. 70A, 114 (1979), Belavin, A.A. and Polyakov, A.M., Pis'ma Zh. Eksp. Torr. Fiz. 22, 503 (1975) [JETP Lett. 22, 245 (1975)].
18. Kawabata, C. and Bishop, A.R., Solid State Commun. 33, 453 (1980).
19. Tyc, S., Halperin, B. and Chakravarty, S., Phys. Rev. Lett. 62, 853 (1989); Chakravarty, S., Halperin, B. and Nelson, D (unpublished).
20. Becker, T. and Reiter, G. (unpublished).
21. Wysin, G.M. and Bishop, A.R. (unpublished).
22. José, J.V., Kadanoff, L.P., Kirkpatrick, S., Nelson, D.R., Phys. Rev. B16, 1217 (1977).
23. Hudak, O., Phys. Lett. 89A, 245 (1982).